# ELASTIC SHOCK RESPONSE AND SPALL STRENGTH OF CONCRETE

**Marlin E. Kipp, Lalit C. Chhabildas and William D. Reinhart**

*Sandia National Laboratories, Albuquerque, NM, USA, 87185-0820**

Impact experiments have been performed to obtain shock compression, release response, and spall strength of two scaled concrete formulations. Wave profiles from a suite of ten experiments, with shock amplitudes of 0.08 to 0.55 GPa, focus primarily on the elastic regime. Despite considerable wave structure that develops as the shock transits these heterogeneous targets, consistent pullback signals were identified in the release profiles, indicating a spall strength of about 30 MPa. Explicit modeling of the concrete aggregate structure in numerical simulations provides insight into the particle velocity records.

## INTRODUCTION

Concrete is a material for which it is desirable to have a comprehensive shock response database in order to assess both local and structural response to projectile impact and explosive loading. The wide range of shock amplitudes that accompany the divergence of a shock from its source requires the acquisition of data over a full spectrum of shock and fracture behavior. The presence of interfaces in the vicinity of shock sources can induce internal fracture (spall) of the material; in addition, shear failure may also occur during propagation of the compressive shock wave.

In this study of two concrete materials with small scale aggregate, gas gun impact experiments are used to obtain Hugoniot data at pressures in the elastic regime. These data are consistent with existing impact data at higher pressure amplitudes. Spall measurements obtained from these low pressure experiments, under the confinement of uniaxial strain, provide insight into one aspect of the fracture response of these two concrete formulations.

In addition, numerical simulations of the impact experiments are reported in which the heterogeneous structure of the concrete is explicitly modeled.

## CONCRETE DESCRIPTION

The two concrete formulations considered in the present study - 'SAC-5' and 'CSPC' - differ primarily in the nature of the aggregate (1,2). SAC-5 has a pea gravel and CSPC has an angular gravel, with maximum dimensions of about 10 mm in both cases, constituting about a 40-45% volume fraction of the concrete, and the rest grout. The SAC-5 concrete has a nominal density of 2260 kg/m$^3$ and an ultrasonic longitudinal velocity of 5060 m/s; the CSPC concrete has a density of 2290 kg/m$^3$ and an ultrasonic longitudinal velocity of 5200 m/s. These properties are similar to those of a full scale aggregate concrete (3).

## EXPERIMENTAL CONFIGURATION

The present plate impact configuration consisted of a projectile launched in a 64 mm light gas gun. The projectile was faced with carbon foam ($\rho = 0.2$ g/cm$^3$) and a flat polymethylmethacrylate (PMMA) impactor. The PMMA impactor plates had thicknesses of approximately 4.5 mm and 9.5 mm, and a diameter of 57 mm. The PMMA impacts directly onto the concrete sample, 12.7 mm thick. Velocity interferometric techniques, VISAR, were used to monitor the velocity of the concrete rear surface. A thin (10 μm) aluminum foil on the rear surface of the concrete ensured that local surface roughness did not impair the veloc-

* Sandia is a multiprogram laboratory operated by Sandia Corporation, a Lockheed Martin Company, for the United States Department of Energy under Contract DE-AC04-94AL85000.

ity measurement. The dispersive nature of heterogeneous materials, however, gives rise to non-unique velocity records whose individual character depends upon the location of the monitoring position. Nevertheless, there will be an average shock response that prevails for the bulk behavior of the material.

For the majority of these experiments, the rear surface of the concrete remained free; in two of the experiments, the concrete was backed with a PMMA window to alter the magnitude of the pullback signal relative to the main shock amplitude, providing a complementary measure of the spall strength.

## DATA SUMMARY

The PMMA plate impactor velocities in this series were in the range of 30 to 220 m/s, resulting in compressive stresses of ~ 80 to 500 MPa in the concrete (Table 1). The wave profiles for all ten experiments are shown in Fig. 1a (CSPC) and 1b (SAC-5). Shock rise time rates are nearly uniform across all the experiments; larger amplitudes have correspondingly longer rise times.

Stress and particle velocity must be continuous at the impact interface. Consequently, estimates for the stress, the particle velocity and the shock velocity can be made utilizing the PMMA impact velocity, free-surface particle-velocity measurements and the PMMA equation of state (4) (Table 1). These shock velocity vs. particle velocity data are plotted in Fig. 2, labelled "Elastic", and are seen to be consistent with existing data for this concrete taken at higher pressure levels (1,2). The corresponding Hugoniot stress vs. particle velocity are plotted in Fig. 3, and are seen to be consistent with the elastic modulus expected based on the concrete longitudinal velocity (dashed line).

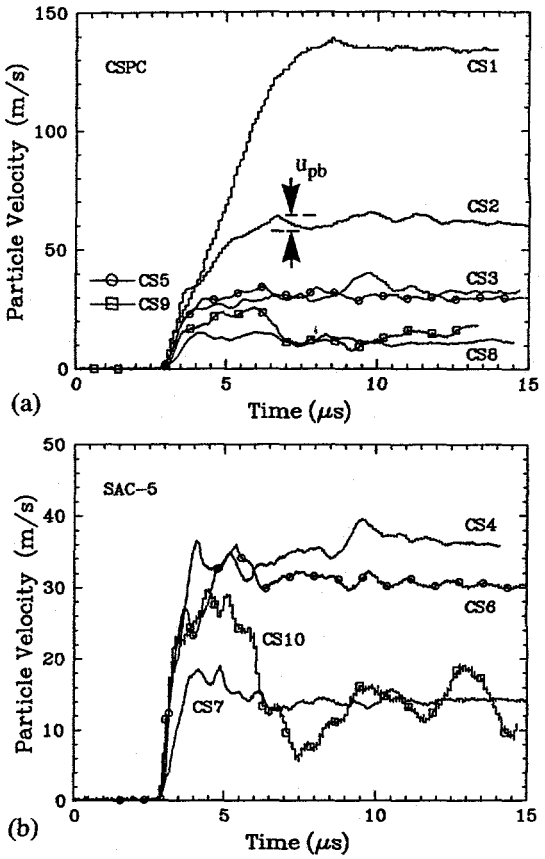


**FIGURE 1.** Particle velocity profiles for CSPC (a) and SAC-5 (b) concrete experiments.

**TABLE 1.** Summary and Results of Impact Conditions.

| Shot | Concrete Type | Target Thickness (mm) | Impactor Thickness (mm) | Impact Velocity (m/s) | Shock Velocity (m/s) | Hugoniot Stress (MPa) | Strain ($u_p/U_S$) (cm/cm) | Spall Stress (MPa) |
|---|---|---|---|---|---|---|---|---|
| CS1 | CSPC | 12.743 | 9.469 | 220 | 3561 | 553 | 0.0191 | 23 |
| CS2 | CSPC | 12.750 | 9.437 | 107 | 3352 | 260 | 0.0101 | 29 |
| CS3 | CSPC | 12.746 | 9.535 | 62 | 3201 | 148 | 0.0063 | 41 |
| CS4 | SAC-5 | 12.753 | 9.528 | 62 | 3299 | 149 | 0.0060 | 15 |
| CS5 | CSPC | 12.753 | 4.427 | 66 | 4334 | 173 | 0.0040 | 29 |
| CS6 | SAC-5 | 12.761 | 4.404 | 62 | 3776 | 155 | 0.0048 | 35 |
| CS7 | SAC-5 | 12.730 | 4.402 | 32 | 3690 | 80 | 0.0026 | 29 |
| CS8 | CSPC | 12.753 | 4.553 | 32 | 5021 | 87 | 0.0015 | 32 |
| CS9 | CSPC/Win | 12.743 | 4.630 | 62 | 4334 | 173 | 0.0040 | 20 |
| CS10 | SAC-5/Win | 12.741 | 4.460 | 62 | 3776 | 155 | 0.0048 | 32 |

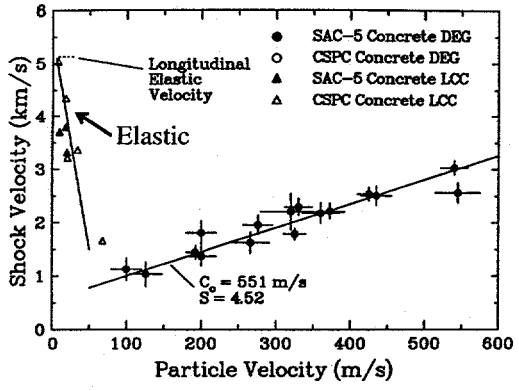


**FIGURE 2.** Shock velocity vs. particle velocity for these experiments ("Elastic", labelled LCC) and existing data at higher pressures (Grady, (1,2) labelled DEG).

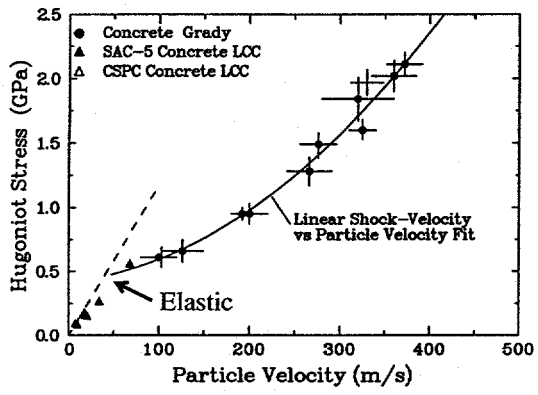


**FIGURE 3.** Hugoniot stress vs. particle velocity for these experiments ("Elastic") and existing data at higher pressures (1,2).

The results for both SAC-5 and CSPC concretes are included in these figures.

Tensile states form within this heterogeneous material when the release waves from the rear projectile surface and target rear surface interact. When the material tensile limit is exceeded, the signal is transmitted to the monitoring surface, where the change in particle velocity ("pullback") indicates the amplitude of the stress level at which fracture occurred (5,6):

$$\sigma_{spall} = \frac{1}{2}\rho c u_{pb} \quad ,$$

where $\rho c$ is the material impedance, and $u_{pb}$ is the pullback velocity for free surface conditions (cf, Fig. 1a). Although the most accurate means of determining the fracture amplitude is to iterate with a one-dimensional shock wave code, so that decay of the signal from the fractured region to the diagnostic surface can be included in the analysis, the current heterogeneity invests the wave profile with sufficient noise as to make such an approach impractical.

Impedance differences between the aggregate and the matrix (grout) result in the development of considerable wave structure as the shock transits the target. Despite the large scale heterogeneous composition of the concrete, consistent pullback signals were identified in the release profiles. It was also determined that attenuation effects in the release waves that define the pullback signal were minimal: when the PMMA impactor thickness was reduced from 9.5 mm to 4.5 mm, thereby changing the location of the fracture region in the sample, no alterations appeared in the particle velocity pullback record.

The spall strength of the concrete for each experiment is listed in Table 1 and plotted as a function of impact Hugoniot stress in Fig. 4. Within the elastic regime, there is some scatter at the lower amplitudes of impact stress, but in general the spall strength appears to be rather constant. The low magnitudes of the fracture stress suggest that the failure is being dominated by the grout or interface bonds, since quartz has a much larger failure stress.

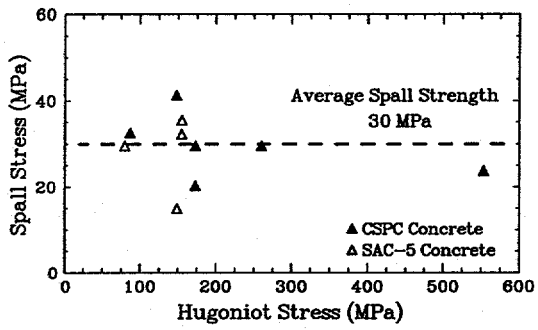


**FIGURE 4.** Spall stress as a function of Hugoniot stress for these experiments.

## NUMERICAL ANALYSIS

The high pressure Hugoniot data included in Figs. 2 and 3 have been utilized in a continuum concrete model developed by Silling (7). The present elastic impact results have motivated numerical simulations in which the target is modeled with explicit aggregate in a grout matrix. An estimated size distribution is used to characterize the dimensions of the aggregate. The position and orientation of each ag-

gregate particle (ellipsoid) is located randomly within a cylindrical envelope that defines the target sample. Similar techniques have been used to define explicit granular structures to explore hot spot formation in explosives (8), and have also been discussed by Amieur, et al (9).

The Eulerian shock-wave propagation code, CTH (10), was used for the simulations. A uniform resolution of 0.2 mm in all three dimensions allowed for about 60 cells through the target thickness. The constituent materials were modeled with a Mie-Gruneisen equation of state and elastic perfectly plastic deviatoric behavior (Table 2).

**TABLE 2.** Material Constants for CTH Simulations.

| Property / Material | Quartz | Grout |
|---|---|---|
| Density, $\rho_0$ (kg/m$^3$) | 2650 | 2000 |
| Bulk Sound Speed, $C_0$ (m/s) | 3760 | 2320 |
| Slope of $U_s$ - $U_p$ Hugoniot, s | 1.83 | 1.68 |
| Gruneisen Coefficient, $\gamma_0$ | 1.0 | 1.0 |
| Specific Heat, $C_v$ (J/kg-K) | 86 | 86 |
| Yield Stress, $Y_0$ (GPa) | 3.1 | 0.5 |
| Poisson Ratio, $\nu$ | 0.18 | 0.22 |
| Fracture Stress, $\sigma_f$ (MPa) | 500 | 30 |

Velocity histories at several spatial locations on the rear surface for the CS6 geometry, obtained from a simulation, are plotted in Fig. 5, and compared with the data. The dispersion and scatter created by the heterogeneous structure of the concrete target is apparent in these records.

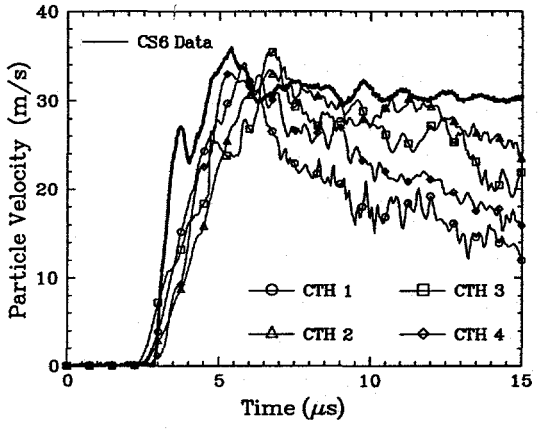


**FIGURE 5.** Numerical simulations of rear surface particle velocity histories compared with experimental data (CS6).

## CONCLUSIONS

The Hugoniot and spall stress have been measured in the elastic regime for two scaled concrete materials. Despite considerable wave structure attributed to the heterogeneous nature of the concrete, the spall amplitudes are quite reproducible, and of nearly constant magnitude over this pressure range. These low pressure shock data are consistent with existing data on these concrete formulations at higher amplitudes. In order to compare with full scale concrete, much larger samples will be required. The current studies were of fully supported shock waves introduced into the concrete. Pulse attenuation studies would also be appropriate to pursue for these materials, to determine how the heterogeneous nature of the concrete influences the decay of the shock. Such data would be important in the simulation of diverging waves in concrete due to projectile impact or explosive loading. It is anticipated that these records will provide additional basis for continued development of damage models for concrete failure.

## REFERENCES


[1] Grady, D. E., "Shock and Release Data for SAC-5 Concrete to 25 GPa", Sandia National Laboratories Technical Memorandum - TMDG0595, October 1995.

[2] Grady, D. E., "Dynamic Decompression Properties of Concrete From Hugoniot States - 3 to 25 GPa", Sandia National Laboratories Technical Memorandum - TMDG0396, February 1996.

[3] Read, H. E. and Maiden, C. J., "The dynamic Behavior of Concrete", *Systems, Science and Software Topical Report* 3SR-707, August 1971.

[4] Barker, L. M. and Hollenbach, R. E., *J. Appl. Phys.*, **41**, 4208-4226 (1970).

[5] Chhabildas, L. C., Barker, L. M., Asay, J. R., and Trucano, T. G., "Spall Strength Measurements on Shock-Loaded Refractory Metals", Shock Compression of Condensed Matter - 1989, Ed. S. C. Schmidt, J. N. Johnson, and L. W. Davison, North-Holland, Amsterdam, 429-432 (1990).

[6] Romanchenko, V. I. and Stepanov, G. V., *Zh. Prikl. Mekh. Tekh. Fiz.*, **4**, 142-147 (1980).

[7] Silling, S. A., "Brittle Failure Kinetics Model for Concrete", in Proceedings of the 1997 ASME Pressure Vessels and Piping Conference, July 27-31, 1997, Orlando, FL.

[8] Baer, M. R., Personal communication, July 1997..

[9] Amieur, M., Hazanov, S., and Huet, C., in "Micromechanics of Concrete and Cementitious Composites", Ed. C. Huet, 181-202, 1993 Presses Polytechniques et Universitaires Romandes, Lausanne.

[10] McGlaun, J. M., Thompson, S. L., and Elrick, M. G., *Int. J. Impact Engng.*, **10**, 351-360 (1990).